Adsorption and Charge-Transfer Study of Bi-isonicotinic Acid on In Situ-Grown Anatase TiO_2 Nanoparticles

Joachim Schnadt,*,† Anders Henningsson,† Martin P. Andersson,‡ Patrik G. Karlsson,† Per Uvdal,‡ Hans Siegbahn,† Paul A. Brühwiler,†,§ and Anders Sandell†

Department of Physics, Uppsala University, Box 530, 751 21 Uppsala, Sweden, Chemical Physics, Department of Chemistry, University of Lund, Box 124, 221 00 Lund, Sweden, and EMPA, Lerchenfeldstrasse 5, 9014 St. Gallen, Switzerland

Received: February 21, 2003; In Final Form: October 13, 2003

Bi-isonicotinic acid (2,2′-bipyridine-4,4′-dicarboxylic acid) is an important ligand in the chemistry of organometallic devices. Here, the adsorption of a monolayer of the molecule on in situ-grown anatase TiO_2 nanoparticles has been investigated by means of X-ray photoemission spectroscopy and X-ray absorption spectroscopy. The bonding geometry is determined to be 2M-bidentate. Furthermore, resonant core spectroscopies have been used to study the excited-state-dependent electron transfer from the core-excited molecule to the substrate. For an excitation to the lowest unoccupied orbital, the excited electron is localized on the molecule because of a core-excitonic effect. Excitation to the two following unoccupied orbitals leads to a charge transfer on a low-femtosecond time scale. This study shows that there is no essential difference in charge-transfer characteristics, compared to the case of adsorption on the rutile (110) surface, for states degenerate with the conduction band.

1. Introduction

The dye-sensitized solar cell represents a class of hybrid materials that have great potential for photovoltaic devices.[1,2] It consists of a mesoporous oxide substrate—most often, anatase TiO_2—that is sensitized to the absorption of visible light via the adsorption of a dye. One of the two most-efficient dyes to date[3,4] is the so-called N3 dye, which is chemically represented as *cis*-$(BINA)_2$-$(NCS)_2$-ruthenium(II), where BINA is bi-isonicotinic acid (2,2′-bipyridine-4,4′-dicarboxylic acid).

The efficiency of the dye-sensitized solar cell is critically dependent on a fast electron injection from the sensitizing molecule into the semiconductor substrate. This coupling, in turn, is, to a large extent, determined by the geometry of the bond to the substrate. A variety of N3 bonding geometries on TiO_2 have been considered, both experimentally and theoretically.[5−9] The general consensus now seems to be that at least a fraction of the carboxylic groups of the dye are deprotonated and bind to the TiO_2 substrate in a bridging (2M-bidentate) geometry.[5] A bond between a second carboxylic group and the substrate leads to further stabilization of the adsorbate complex, especially if a bridging geometry is also realized here.[6] Now, a question arises: does the second carboxylic group belong to the same bi-isonicotinic acid ligand as the first, or is the bonding realized via the second ligand? The latter possibility has been preferred in refs 6 and 8, whereas the former has been suggested in refs 7 and 9. It is difficult to distinguish experimentally between these two cases, because there is, a priori, no simple way of deciding which carboxylic groups are participating in the bonding. However, model adsorption studies of the bi-isonicotinic acid ligand on TiO_2 substrates can determine whether a geometry that involves both carboxylic groups of a single ligand is feasible or not.

In a previous study of the adsorption of bi-isonicotinic acid on a rutile $TiO_2(110)$ single-crystal surface, we found that such a bidentate bonding geometry that involves both carboxylic groups is the optimal one.[10] In a second step, the coupling strength of the adsorbate to the substrate was studied, and it was determined to be so strong that an electron transfer from the molecule to the substrate could occur in <3 fs.[11] In the present study, the adsorption of bi-isonicotinic acid on an ultrahigh vacuum (UHV) in situ-prepared film of anatase TiO_2 nanoparticles is investigated. This substrate has recently been characterized;[12] a scanning tunneling microscopy (STM) image of the substrate is shown in Figure 1. The anatase phase and the granular morphology of the film makes it more similar to the nanoporous TiO_2 structure that is used in the solar cell than the rutile single crystal of the previous study. Hence, the present results should be more applicable to the real system, while the ultracleanliness of the UHV environment is preserved. It will be shown that, in correspondence to the rutile single-crystal case, a bridging bonding geometry that involves both carboxylic groups is realized, despite the differing geometrical constraints exerted by the surface. Furthermore, resonant photoemission spectroscopy (RPES) and resonant Auger electron spectroscopy (RAES) have been used to study the state-dependent electron transfer from the core-excited molecule to the substrate.[14] The present case is quite similar to the RPES study of bi-isonicotinic acid on rutile $TiO_2(110)$,[11] and it will be shown here that an electron transfer from states that are degenerate with the conduction band also occurs on a low-femtosecond time scale. This result agrees well with a similar RAES investigation of injection times from N3 into nanoporous TiO_2.[15]

* Author to whom correspondence should be addressed. E-mail: achim@phys.au.dk. Present address: Department of Physics and Astronomy, University of Aarhus, Ny Munkegade, 8000 Aarhus C, Denmark.
† Uppsala University.
‡ University of Lund.
§ EMPA.

10.1021/jp0344491 CCC: $27.50
Published on Web 02/11/2004

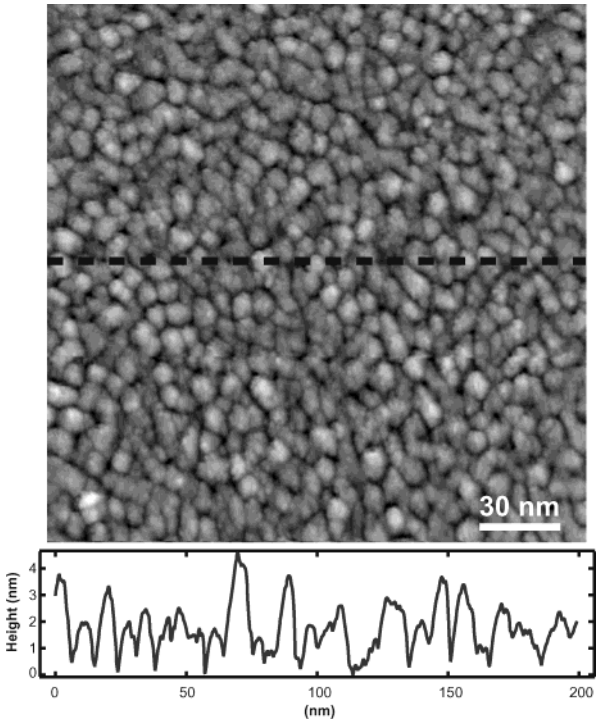

Figure 1. Ultrahigh vacuum scanning tunneling microscopy (UHV−STM) image of a representative, in situ-grown TiO_2 film (taken from ref 12). A detailed characterization of the film is given in ref 12. The dashed line in the upper panel defines the path used to produce the profile in the lower panel. The particle size is ∼10 nm, which is comparable to the crystallite radius of the nanoporous TiO_2 film that is used as the standard in the dye-sensitized solar cell.[13]

2. Experimental Section

The X-ray photoemission spectroscopy (XPS) and X-ray absorption spectroscopy (XAS) experiments were performed at Beamline D1011[16,17] at the Swedish synchrotron radiation facility MAX-Lab in Lund, Sweden. The sample preparation was conducted in situ under UHV conditions (the base pressure in the preparation chamber was in the low-10^{-10} Torr range, and in the low-10^{-11} Torr range in the analysis chamber). The anatase film growth procedure and characterization are described in ref 12. Bi-isonicotinic acid was sublimated onto the anatase nanoparticle film in situ, as in the rutile single-crystal study,[10] and care was taken that the coverage did not exceed one monolayer (see below). The photoemission spectra were referenced to the energy of the vacuum level (E_{Vac}).[18] The photon energies of the X-ray absorption spectra were calibrated by measuring the kinetic-energy difference of a core-level photoemission line, using first- and second-order light. For the purpose of imaging the core-excited density of states, they were furthermore placed onto the same scale as the photoemission spectra, as outlined in refs 14 and 19. The kinetic-energy scale of the Auger spectrum was calibrated by referencing it to the calibrated kinetic energy of a characterized core level. The X-ray absorption spectra were taken at intervals of ∼0.1 eV, and the resonant photoemission spectra were obtained with a photon energy resolution of 0.3 eV. The latter value is much larger than the N 1s lifetime broadening of ∼0.11 eV,[20] which means that the experiment is conducted in the broad-band excitation limit.

3. Results

3.1. Bonding Geometry. The major aspects of the bonding geometry of bi-isonicotinic acid on the nanostructured anatase TiO_2 film are very similar to those found for bi-isonicotinic acid on a rutile TiO_2(110) single-crystal surface.[10,21] The O 1s X-ray photoemission spectrum is shown in Figure 2. It exhibits two peaks, at 534.4 and 535.9 eV. The intensity ratio between these two peaks varies with the amount of bi-isonicotinic acid. From a series of such experiments, and from the similarity to the rutile system (cf. Figure 2), the peak at 534.4 eV is assigned to emission from the TiO_2 substrate O atoms. The high-binding-energy peak stems from the O atoms of the bi-isonicotinic acid molecule. Clearly, only one molecular peak is found in the spectrum, whereas the O 1s spectrum for a multilayer of bi-isonicotinic acid (cf. Figure 2 and ref 10) exhibits two well-separated molecular features (the peak at ∼535 eV in the multilayer spectrum is due to photoemission from the substrate and is visible here because of the limited thickness of the multilayer, ca. 20 Å). This shows that the molecular O atoms are inequivalent in the multilayer, because of the presence of the carboxylic H atom. In contrast, the presence of the substrate

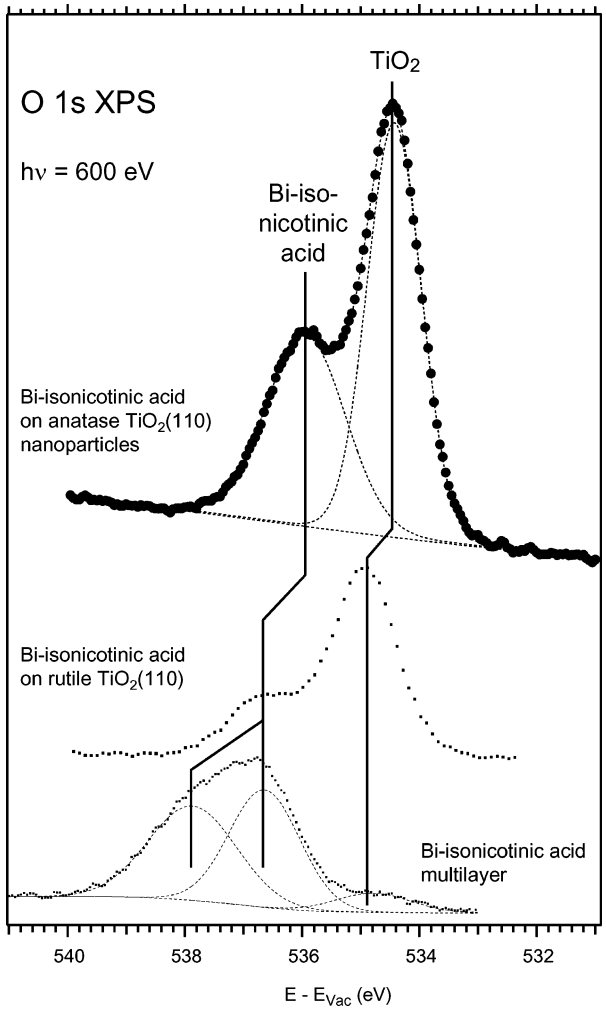

Figure 2. O 1s X-ray photoemission spectra for monolayers of bi-isonicotinic acid on anatase TiO_2 nanoparticles and, for comparison, bi-isonicotinic acid on rutile TiO_2(110).[10] In addition, the spectrum for a multilayer of bi-isonicotinic acid[10] has been given. The monolayer spectrum of the anatase sample exhibits two peaks: the lower-energy peak is ascribed to emission from the substrate atoms, and the higher-energy peak stems from the carboxylic O atoms. The occurrence of only one molecular peak, in contrast to two, chemically shifted peaks for the multilayer case, suggests the equivalency of the molecular O atoms and, thus, a deprotonation of the carboxylic groups and an involvement of all four O atoms in the bond to the substrate. Thus, the present case is observed to be to parallel that of bi-isonicotinic acid on rutile TiO_2(110), which has a similar O 1s spectrum.

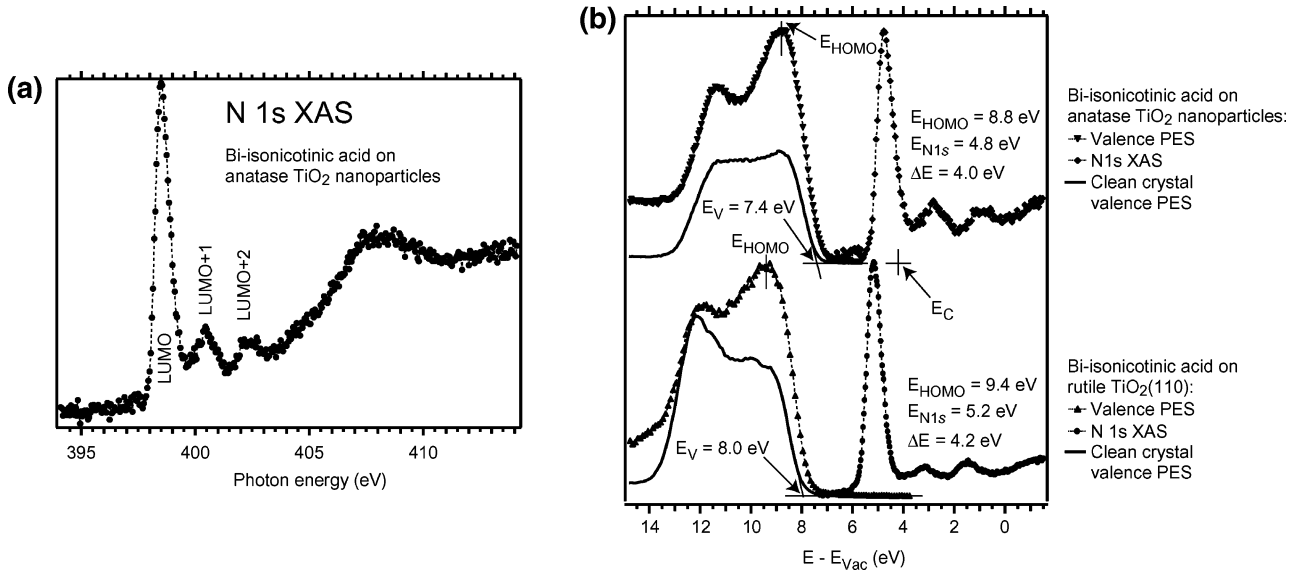

Figure 3. (a) N 1s X-ray absorption spectrum for a monolayer of bi-isonicotinic acid on the anatase film. (b) Valence electronic structure of the bi-isonicotinic acid on the anatase film (upper curve) and on rutile TiO_2(110) (lower curve).[11] Here, valence photoemission and X-ray absorption spectra have been placed on a common ionization potential scale.[14,19] The E_V notation indicates the valence-band edge in each case, whereas the E_C notation marks the estimated conduction-band edge for the anatase sample. The E_{N1s} notation gives the energies of the lowest unoccupied state, as observed in the X-ray absorption spectrum, whereas the E_{HOMO} notation marks the position of the highest occupied molecular orbital (HOMO).

and only one molecular component in the monolayer spectrum indicates the chemical equivalency of the four molecular O atoms.[10] We interpret this phenomenon in terms of a deprotonation of the carboxylic group and a substrate bonding that occurs via the four O atoms of the carboxylic groups. Interestingly, the substrate O 1s peak is narrower than both the molecular peak and the corresponding peak in the rutile spectrum. This could be explained by different vibrational broadenings for the different substrates and for the different oxygen species. In view of the differences between the rutile and anatase nanoparticle substrate geometries, this would be quite plausible. Alternatively, it is possible that the different oxygen species in the anatase system are more similar to each other chemically than in the rutile system and, furthermore, that they are more similar to each other than the molecular O atoms. This slight inequivalency of the latter could then be explained by the strain exerted by the substrate bond; however, it would be less severe than the inequivalency induced by the presence of a proton that is bound to the carboxylic group. Therefore, we conclude that this aspect of the bonding configuration is the same in the rutile and anatase nanoparticle cases; i.e., the bonding geometry is 2M-bidentate for both carboxylic groups, which supports earlier calculations.[9]

Having established the nature of the two features in the O 1s spectrum, we can make a crude estimate of the amount of bi-isonicotinic acid that has been sublimated. The observed intensity ratio of the two peaks in the spectrum corresponds approximately to a saturated monolayer, which can be deduced from the fact that it was not possible to sublimate more molecules without obtaining a third peak in the spectrum. It is difficult to specify the coverage in more detail, i.e., in terms of molecules per unit cell, because the exact structure of the nanoparticles of the present film, in terms of surface orientations, is not yet known. It is likely that (i) the (101) orientation is the most prominent one, because of its enhanced stability, compared to other low-index orientations,[22,23] and (ii) it is not reconstructed.[24,25] Alternatively, the film could consist of rodlike particles with a predominance of (100) faces. However, the morphology (cf. Figure 1) with a small degree of order suggests that this is not the case.[26] Assuming that the (101) surface is the most important one, some conclusion can be drawn from the recent calculations that have been mentioned previously.[9] The preferred geometry found there implies that there is a bond to each of the 5-fold-coordinated Ti atoms of the surface if the molecules are closely packed. In this model, the surface can accommodate one molecule per surface unit cell.

We now consider the N 1s X-ray absorption spectrum, which shows the unoccupied molecular orbitals with weight on the N atom in the presence of the N 1s core-hole originating from the excitation (cf. Figure 5e later in this paper). The spectrum in Figure 3a contains the following three sharp resonances: the lowest unoccupied molecular orbital (LUMO), the LUMO+1 resonance, and the LUMO+2 resonance, at 398.5, 400.5, and 402.4 eV, respectively, and, in addition, a large σ-shaped resonance-like feature at ~408 eV. These positions are almost identical to those found for bi-isonicotinic acid on rutile TiO_2-(110) (398.7, 400.5, and 402.4 eV, respectively), which indicates that the unoccupied orbitals probed in the two cases are very similar. For bi-isonicotinic acid on rutile TiO_2(110), it has been shown that the LUMO+1 orbital results from an orbital that, for the isolated molecule, lies higher in energy than the LUMO+2 orbital but is drawn down to a position between the LUMO and LUMO+2 resonances by the substrate interaction.[27] The fact that almost the same energy position is observed in the present case indicates a similar bonding interaction in the rutile and anatase systems.

In regard to the core-level photoemission spectra (cf. Table 1 and Figures 2 and 4), an overall shift between 0.4 eV and 0.7 eV to lower binding energies is observed when changing from the rutile single-crystal surface to the anatase nanoparticle film. This shift is attributed to a different work function and a different core-hole screening behavior, which are due to the differing substrate geometries.

Figure 4 shows that the main peak of the N 1s core-level line for a monolayer preparation follows this trend, whereas the shake-up structure[28] at higher binding energies shifts by a considerably larger amount. Thus, the separation of the shake-up structure is changed, compared to the main peak structure.

TABLE 1: Ionization Potentials for Bi-isonicotinic Acid Monolayers on the Indicated Substrates[a]

	O 1s		N 1s		C 1s	
substrate	molecule	substrate	main peak	shakeup	main peak	carboxylic
anatase nanoparticles	535.94	534.43	403.27	405.88	289.70	293.06
rutile TiO_2(110)	536.62	534.99	403.84	407.02	290.09	293.57
Δ	−0.68	−0.56	−0.57	−1.14	−0.39	−0.51

[a] All values given in eV. The experimental uncertainty is ±0.05 eV for the ionization potentials and, accordingly, is ±0.07 eV for the differences.

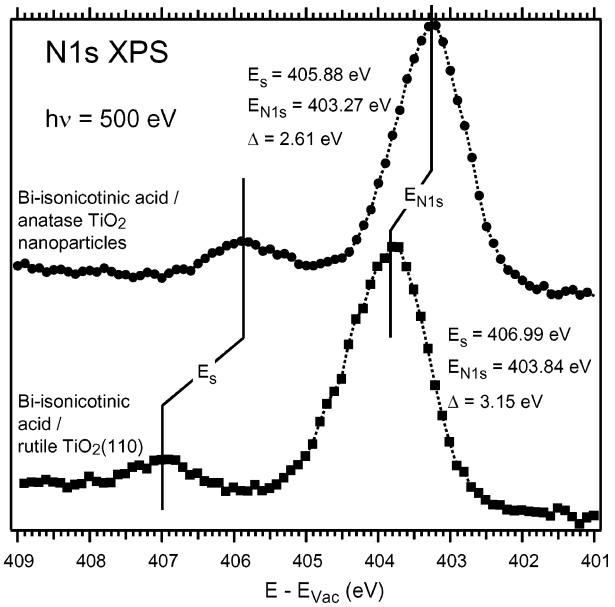

Figure 4. N 1s photoemission spectra for monolayers of bi-isonicotinic acid on rutile TiO_2(110) (lower curve) and the present preparation on the nanostructured film. The main line of the rutile preparation lies at an ionization potential that is ∼0.6 eV higher than that in the present case; a similar shift is observed for all core levels and can be attributed to a different net contact potential and/or surface dipole of the monolayer-covered nanostructured film, compared to the rutile single-crystal (110) surface. The numbers given in the figure correspond to the binding energies of the main and shake-up peaks and have error margins of ±0.05 eV. E_S is the shake-up energy, and E_{N1s} that of the main line; Δ represents the difference between both energies.

For the anatase nanoparticle case, the difference between the main line and the shake-up is $\Delta = 2.61$ eV ± 0.05 eV, whereas it is $\Delta = 3.15$ eV ± 0.05 eV for the rutile substrate. We assume that this particular shakeup primarily involves charge redistribution (i.e., an electron transfer) between the two rings, as for biphenyl,[30] although the substrate interaction also must have an important role. The latter point can be deduced from two observations, namely, that (a) the shake-up structure is not present in N 1s spectra taken on multilayer preparations of bi-isonicotinic acid[32] and (b) a similar, but much weaker, shake-up structure is found for monolayer preparations of the pyridine−carboxylic acid monomers.[32]

The closer proximity of the shake-up peak to the main peak for the bi-isonicotinic acid/anatase TiO_2 sample is accompanied by a similar narrowing of the HOMO−LUMO gap, which, however, as indicated in Figure 3, only amounts to ∼0.2 eV, as compared to ∼0.5 eV for the shake-up energy. For an isotropically charge-neutral ground state, the energy of a given shake-up transition is given by the Coulomb energy of the final-state charge distribution, which can often be estimated approximately, given some knowledge of the distribution of the relevant wave functions. Therefore, we make the crude assumption that the aromatic bi-isonicotinic acid molecule is almost nonpolar. Concentrating on the lowest shake-up energy of biphenyl,[30] and examining the lowest shake-up transition there, we estimate the relevant wave functions to have a mean separation of 8.6 Bohr radii and assume that a similar value should describe BINA. Thus, their attractive Coulomb interaction will amount to ∼3.16 eV, which is in good agreement with the observed shake-up energy for biphenyl, but also with that of BINA on rutile (110). This observation suggests that the orbital reorganization and substrate screening for BINA/rutile (110) compensate each other, to the extent that the present approximate estimate for an isolated molecule is accurate. When analyzed in the same terms, the shake-up energy for BINA adsorbed on the anatase nanoparticles would imply a separation of ∼10.4 Bohr radii. A corresponding change of 1.8 Bohr radii in the separation between the two pyridine rings would lead to a breaking of the inter-ring bond and, thus, the disappearance of the shake-up feature. Thus, the change in energy separation between the main and the shake-up peaks cannot be explained by a corresponding change in the inter-ring distance; therefore, we conclude that effects that are due to the substrate must be included in an explanation,[33] which is consistent with what has been said previously. This is further supported by calculations[9] of the bonding geometry of bi-isonicotinic acid on anatase TiO_2-(101), which show that the inter-ring distance is not affected by the substrate geometry.

3.2. Charge-Transfer Dynamics. Resonant core spectroscopies can be used to probe the interfacial charge-transfer dynamics of the core-excited system in the low- and sub-femtosecond (sub-fs) time regimes.[14] A schematic outline of the different techniques used here is presented in Figure 5, with ordinary (nonresonant) photoemission and Auger spectroscopies in panels a, b, and d, and XAS in panel e. The latter also corresponds to the excitation step of the resonant core spectroscopies, which are given by the two electronic de-excitation channels in panels f and g. The de-excitation channels differ in that resonant photoemission spectroscopy (RPES, panel f) monitors only decay events in which the excited electron participates (these events are often termed "participant decays"), whereas resonant Auger spectroscopy (RAES, panel g) monitors all other electronic decay channels (often called "spectator decays"). The electronic decay of the core-excited system is characterized by the core-hole lifetime τ_C,[39] which, in our case (N 1s core-hole), is taken to be 6 fs. A comparison of panels a and f in Figure 5 shows that nonresonant valence photoemission and RPES have the same final state. Thus, a resonant photoemission spectrum is recorded by measuring the valence photoemission spectrum around the absorption edge that is defined by the X-ray absorption spectrum in panel e in Figure 5 and integrating its intensity (see, for example, refs 14 and 40). RAES occurs at somewhat larger binding energies, which can be rationalized from the similarity of the RAES and valence shake-up final states (cf. panel c in Figure 5). For broad-band excitation, RAES disperses on the binding energy scale with the photon energy (i.e., has a constant kinetic energy), whereas RPES is constant, in regard to binding energy.[41] In principle, this allows a separation of the RPES and RAES spectral contributions, which, however, is not always trivial, particularly for the lowest relevant photon energies.

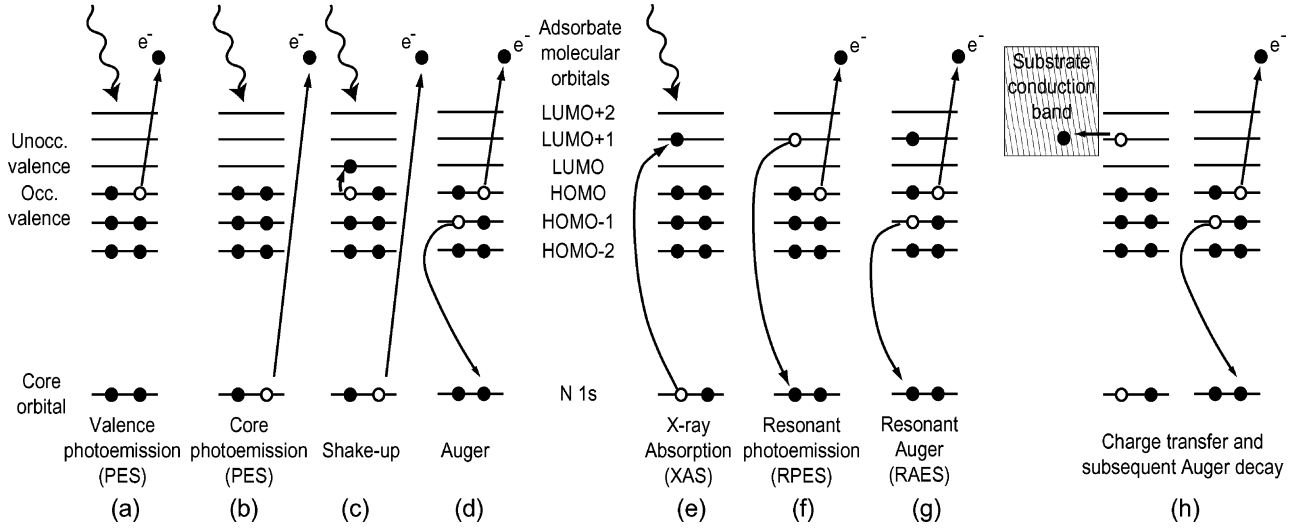

Figure 5. Spectroscopic techniques used in the present study and corresponding processes; the horizontal lines indicate molecular orbitals, the filled circles represent electrons, and the open circles denote holes (missing electrons). The core level used here was the N 1s level. Panels a−d represent nonresonant processes, whereas panels e−g represent resonant processes (as applied to an isolated molecule). Panel h shows that when a substrate continuum is coupled to the molecule, charge transfer and subsequent Auger decay may compete with the resonant decay channels in panels e and f.

When a substrate continuum is coupled to the molecular system, a transfer of the excited electron into the substrate on a femtosecond time scale and a subsequent "normal" Auger decay (panel h in Figure 5) may compete with the resonant decays of RPES and RAES, which are then reduced in intensity, in favor of the normal Auger intensity. In the RPES mode, a comparison of the RPES to the XAS signal can be used to estimate the electron-transfer time.[14] In particular, for the LUMO+1 and the LUMO+2 resonances of N 1s core-excited bi-isonicotinic acid, the charge-transfer time scale can be estimated from the spectral XAS and RPES intensities, from[11,40]

$$\tau_T = \left[\frac{I_{RPES}/I_{XAS}}{\sigma - (I_{RPES}/I_{XAS})}\right]\tau_C$$

The factor $\sigma = 0.3$ gives the ratio of the RPES intensity to the XAS intensity for the LUMO+2 resonance in the bi-isonictonic multilayer (cf. Figure 6b), which serves as a representative for the isolated molecule without charge transfer.[11,40] Hence, the multilayer provides a necessary calibration for the RPES intensity, with respect to that of the XAS signal.[43]

Furthermore, the indicated procedure relies on a proper intensity normalization of the RPES signal, relative to the X-ray absorption spectrum. In Figure 3b, where the valence photoemission and the X-ray absorption spectra have been placed on a common energy scale, the LUMO at a photon energy of 398.5 eV is observed to be situated almost completely within the substrate band gap. In the figure, the optical gap of the TiO_2 substrate (3.2 eV) has been indicated by marking the valence band and conduction band edges, and the figure shows that the LUMO lies ~0.7 eV below the latter. Calculations show that the (ground-state) LUMO is expected to overlap the conduction band.[44] The present location within the band gap, as measured by XAS, is due to a core-excitonic effect, i.e., a reduction of the orbital energy that is due to the additional Coulomb attraction exerted by the N 1s vacancy.[27,45] Thus, any charge transfer from the LUMO to the substrate conduction band on the femtosecond time scale is energetically forbidden for this particular state, and the resonant photoemission and X-ray absorption spectra can be normalized to the height of this resonance.

A comparison of the normalized RPES and XAS curves is presented in Figure 6a. The RPES intensities are clearly reduced, relative to those of the X-ray absorption spectrum for excitation to the LUMO+1 and LUMO+2 orbitals, and they are much smaller than the corresponding intensity in the multilayer RPES for the LUMO+2 resonance, for which the excited electron is localized on the bi-isonicotinic acid molecule (cf. Figure 6b). The present noise level, in comparison to the intensity of the XAS resonance, does not allow an evaluation at the LUMO+2 resonance, but for the LUMO+1 resonance, we are able to estimate the peak intensity in the RPES—$I_{RPES}/I_{XAS} \lesssim 0.16$—which leads to $\tau_T \lesssim 6.9$ fs. However, to achieve a reasonable noise level, the valence-band intensity has been integrated between 7.0 eV and 12.2 eV (cf. Figure 3b), possibly leading to a significant normal Auger/RAES contribution. This, and the fact that the signal has been estimated rather conservatively, with respect to the noise, means that the given value should be viewed as a conservative upper limit on the charge-transfer time.

As outlined previously, the other approach to the measurement of a charge-transfer time is to monitor all electronic decay events and identify the normal Auger and RAES contributions to the spectrum.[14,46] In that case,

$$\tau_T = \frac{I_{RAES}}{I_{Auger}}\tau_C$$

Although the RAES signal is quite similar in shape to that of the normal Auger signal, it can often be distinguished from the latter by virtue of the so-called spectator shift.[47] (As mentioned previously, the resonant Auger event is often called the spectator decay process, because the excited electron does not participate in the decay.) The excited electron screens the positive core-hole, and, thus, the resonant Auger signal is found at higher kinetic energies (hence, lower ionization potentials) than that of the normal Auger signal. This is illustrated in Figure 7a. Here, the resonant signal (which is comprised of RPES and RAES) at approximately the photon energy of the LUMO (398.4 eV) is compared to a curve that represents the Auger spectrum (solid gray curve). Disregarding the peaked RPES and direct photoemission features, the resonant and Auger spectra are in good

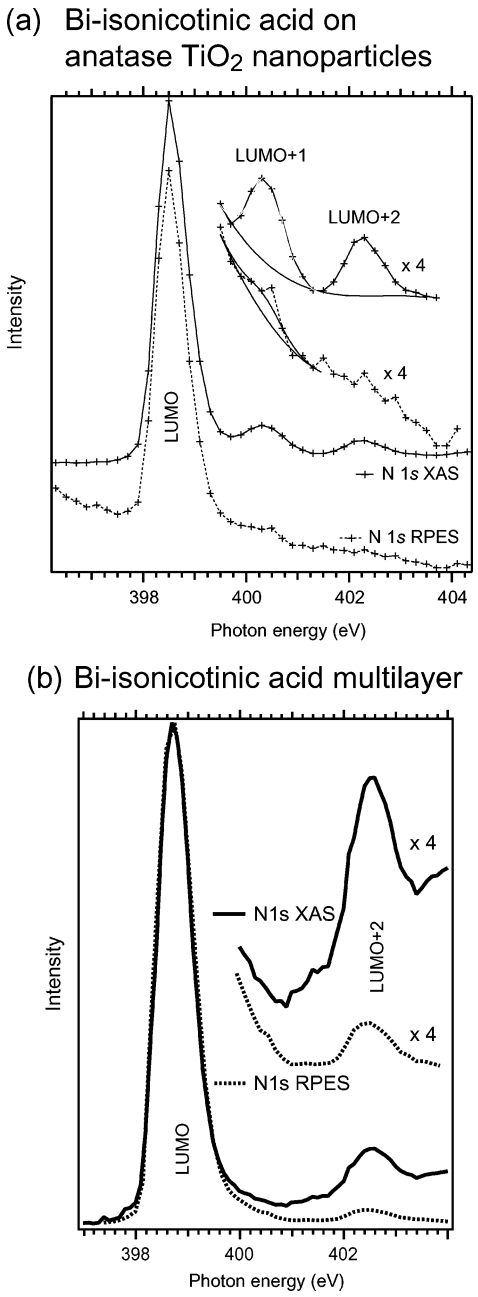

Figure 6. (a) Comparison of the XAS to the RPES used to derive charge-transfer time limits for the present case of a monolayer of bi-isonicotinic acid on anatase TiO_2 nanoparticles. The intensity of the LUMO+1 RPES signal was fitted with a Gaussian, taking the indicated baseline into consideration. The fit corresponds then to ~16% of the XAS LUMO+1 intensity. (b) For comparison, the X-ray absorption and resonant photoemission spectra for the bi-isonicotinic acid multilayer[40] are shown here. The X-ray absorption spectrum consists of two peaks only, which are labeled LUMO and LUMO+2. This appearance of an additional peak (LUMO+1) in the monolayer spectrum in panel a can be explained from a downward shift of the concerned level from a position above the LUMO+2 when the substrate bond is formed.[27] The resonant photoemission spectrum clearly exhibits intensity not only for the LUMO, but also for the LUMO+2 orbital, which is due to a localization of the excited electron on the molecule (see text).

agreement when the latter is shifted by ~3 eV to higher kinetic energies (solid black curve). This value is in reasonable agreement with the LUMO spectator shifts of condensed benzene (~3 eV to 4 eV),[48] pyrrole (~2.5 eV at the C K-edge and ~4.0 eV at the N K-edge),[49] furan (~4 eV),[49] and condensed pyridine, pyrazine, and s-triazine (~4.0 eV).[50] However, note that, for the particular case of a monolayer of bi-isonicotinic acid on TiO_2, it is nontrivial to measure the Auger spectrum for an excitation of the N 1s electron (the so-called N KVV Auger spectrum). The present curve has been extracted from 51 different curves,[51] and this procedure seems to overestimate the Auger intensity for kinetic energies higher than ~384 eV (387 eV for the estimated spectator curve). This can be deduced from the argument that the onset of spectator intensity should maintain a minimum separation to the highest-kinetic-energy RPES feature which corresponds to the HOMO−LUMO gap. Figure 3b indicates that this separation amounts to at least 2 eV (measured base-to-base). This is clearly not the case for the spectator curve presented in Figure 7. Nevertheless, the good agreement of the principal shapes at lower kinetic energies, as well as the good agreement with the spectator shifts of other aromatic molecules discussed previously, lend support to the present estimate.

A similar comparison was also undertaken for excitation to the LUMO+1 and LUMO+2 resonances (cf. Figure 7b and 7c). In both cases, the main portion of the spectrum is explained well by normal Auger spectroscopy and direct photoemission; note that the resonant parts of the spectrum are much smaller than those in the LUMO case, because of the smaller absorption cross section in the X-ray absorption spectrum. To estimate the maximum share of the resonant Auger signal, the decay signal was modeled by a sum of the normal Auger curve and a shifted one, which represented the RAES curve. Using the same spectator shift as that for the LUMO resonance, the ratio of the RAES intensity to the normal Auger intensity, I_{RAES}/I_{Auger}, was observed to lie well below 10% for the LUMO+1 resonance and well below 25% for the LUMO+2 resonance. However, the spectator shift is state-dependent and is expected to be smaller for the higher resonances.[50,52] Measurements on thick films of bi-isonicotinic acid (not shown here) suggest that the spectator shift is decreased by ~1 eV when passing from the LUMO orbital to the resonance, which corresponds to the LUMO+2 resonance of the monolayer. Figures 7b and 7c give an estimate for the maximum share of the RAES intensity for the LUMO+1 and LUMO+2 resonances for this shift. For the LUMO+1 resonance, we find $I_{RAES}/I_{Auger} < 25\%$, resulting in $\tau_T < 1.5$ fs. For the LUMO+2 resonance, the ratio is larger and corresponds approximately to the limit of the RPES measurement: $I_{RAES}/I_{Auger} < 115\%$ and $\tau_T < 6.9$ fs, irrespective of whether the spectator shift is chosen to be 1.5 or 2 eV. The latter ratio limit is also observed for the LUMO+1 resonance when the spectator shift is reduced to ~1.5 eV.

Clearly, the latter method of estimating the charge-transfer time is rather approximate, because of the difficulties in distinguishing between the normal Auger and resonant Auger components of the spectrum. Together with the RPES measurement, however, they give us confidence that, for both the LUMO+1 and LUMO+2 resonances, the transfer time lies below 7 fs. For the LUMO+1 resonance, it actually should lie well below this limit. The results for the 2-eV spectator shift suggest that it may even lie in the sub-femtosecond regime.

4. Discussion

There are several points that should be discussed more thoroughly, to clarify the bearing of the present X-ray results on valence-excited systems. These concern the size of excitonic effects and the spatial and temporal scales of the different excitation modes.

First, the position of the LUMO within the band gap raises the question of the validity of a comparison of the present

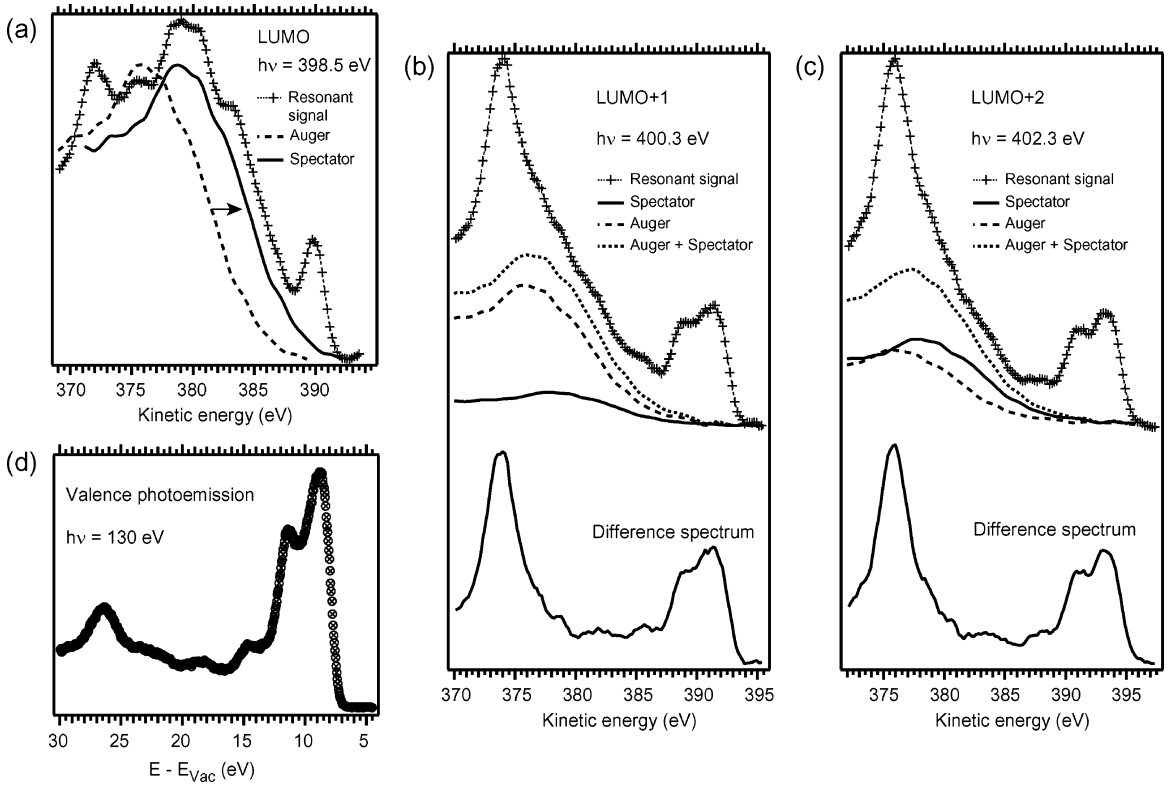

Figure 7. Resonant Auger electron spectra for the three lowest unoccupied states found in the XAS analysis. The resonant portion of the spectrum is modeled using a nonresonantly measured Auger curve. In panel a (for LUMO), the bulk of the intensity is well-described by an Auger curve that is shifted by 3.0 eV (spectator shift). The shifted curve is labeled "Spectator". The remaining intensity is ascribed to RPES and direct photoemission. In panels b (for LUMO+1) and c (for LUMO+2), the main component of the intensity can be modeled by the normal Auger curve. A shifted (resonant) component has been taken into consideration by adding an Auger curve that is shifted by 2.5 eV. Here, the intensity of the shifted components amounts to 25% of that of the nonshifted ones for the LUMO+1 resonance and 115% for the LUMO+2 resonance. The lower portions of the graph show the difference spectrum of the resonant curve and the two Auger components, nicely reproducing the nonresonant valence photoemission spectra in panel d, aside from expected changes in the relative cross sections.

X-ray measurements and optical experiments. Although recent calculations[53] seem to indicate that the lowest excited state of the valence-excited system overlaps the conduction band, a compilation of relevant experimental values shows that core and valence excitonic effects can have very similar sizes in systems with efficient electronic screening.[54] Bi-isonicotinic acid with its extended π-systems falls into this class of molecules; hence, we expect the LUMO of the valence-excited system to lie within the band gap. However, this expectation must be checked experimentally. Because the present results show that the molecular adsorbate bonds strongly enough to the TiO_2 substrate to allow an electron transfer within a few femtoseconds, they are, in any case, at least indirectly relevant, even to the valence-excited system. Even these systems will be characterized by strong substrate bonding, which makes ultrafast electron transfer possible. Furthermore, calculations[27] indicate that the higher resonances are easily decomposed to the ground-state basis, showing that the core-hole is a moderate perturbation for the higher states. A more-thorough discussion of this point is included in ref 40.

Second, both the spatial nature and the light frequency of X-ray excitations are different from those of valence excitations. Because of their chemical specificity, the former are very local, with a characteristic lengthscale of a single atom and a frequency that corresponds to the length of a single electromagnetic wave cycle in the attosecond (10^{-18}) regime (i.e., much shorter than the transfer time scale). This contrasts with the case of valence excitations, in which the characteristic spatial extent is given by that of the molecular valence states, and the light frequency corresponds to a time scale that is comparable to that of the transfer itself. As already stated previously, however, the rapid screening response mediated by the molecular π-system on the electron-transfer time scale renders the spatial characteristics very similar in both cases, and they are defined by the sizes of the adsorbate molecular orbitals (cf. refs 27 and 53). The degree of hybridization of these orbitals with the substrate conduction band then determines the time scale of the electron transfer, which proceeds in the electronic limit.[55] In both cases, the transfer can be viewed in terms of a continuous development of the wave functions. In the valence-excitation case, this development proceeds on a time scale that is comparable to or shorter than the time scale of the wave cycle. The much-shorter time scale of the X-ray experiments is then an advantage, in principle, because it makes it possible to truly probe the ultrafast electron transfer with access to faster molecular dynamics.[14] Here, the charge transfer is so fast that these dynamics are apparently quenched, and only the core-hole lifetime is important, giving access to the magnitude of the transfer bandwidth.

From this discussion, we conclude that, although there are distinct differences between X-ray and optical measurements, the present results have an important impact on the understanding of electron transfer in strongly coupled adsorbate−oxide systems and, in particular, have an important impact on the rationalization of the ultrafast charge transfer in systems of chromophores that are anchored to a nanostructured TiO_2 substrate via one or more carboxylic groups.

5. Conclusions

The adsorption and core-excited charge-transfer characteristics of bi-isonicotinic acid on a nanostructured anatase TiO_2 film have been studied. This system models closely the interface between the dye and the TiO_2 substrate in the dye-sensitized solar cell. Both the adsorption geometry and the core-excited charge-transfer characteristics are very similar to those of bi-isonicotinic acid adsorbed on a rutile TiO_2(110) single-crystal surface. The substrate bond has been determined to be formed in a 2M-bidentate geometry via both carboxylic groups of the molecule. The form of the X-ray absorption spectrum suggests that the bond is of a similar strength and molecular configuration as that in the corresponding rutile system, and, thus, the validity of the rutile model system is confirmed. This finding is further supported by the results of the resonant photoemission and resonant Auger measurements. The lowest resonance is situated within the band gap, because of a core-excitonic effect, so that any femtosecond electron transfer from the molecule to the substrate is electronically forbidden, whereas the second and third resonances couple so strongly to the substrate that the excited electron is transferred on a time scale of a few femtoseconds.

These results cannot prove that N3 binds to the nanocrystalline substrate of the solar cell with both carboxylic groups of a single ligand in a 2M-bidentate fashion; however, they show that this possibility is feasible. The study gives an experimental confirmation of the theoretical expectation that the bi-isonicotinic acid ligand is able to respond to the constraints imposed by the anatase geometry and form strong chemical bonds to the substrate with both carboxylic groups.[27] Future investigations will have to clarify the geometric influence of the bonds between the metal center of the N3 complex to the bi-isonicotinic acid ligand.

The findings from the resonant photoemission spectroscopy/resonant Auger spectroscopy (RPES/RAES) investigations show clearly—in particular, for the LUMO+1 resonance—that the carboxylic groups form a negligible barrier for the charge-transfer process, significantly extending the basic thesis of the previous work[10,11,27] on rutile (110), in regard to the role of the coupling of the ligand for the function of solar cells based on N3 adsorbed on nanostructured TiO_2. For $Ru(bpy)_2(BINA)^{2+}\cdot 2PF^-_6$ (bpy is bipyridine and BINA is bi-isonicotinic acid), which is a complex that is quite similar to N3, the charge transfer from the LUMO+2 resonance has been determined to be slower than that in the case of bi-isonicotinic acid on rutile.[15] This delay has been ascribed to an intramolecular electron delocalization with the excited electron spending time on the other two bipyridine ligands and must also include the effects of N 1s excitation on the nonsubstrate-bound ligands, which will lengthen the measured transfer time. The results reported here support such an interpretation, because the bi-isonicotinic acid adsorbate—anatase substrate coupling is determined to have a strength that is similar to that of the corresponding bond in the rutile system.

Acknowledgment. We would like to acknowledge the staff of MAX-Lab, and our funding sources Vetenskapsrådet, Göran Gustafssons Stiftelse, and the CARAMEL Consortium, which is funded by Stiftelsen för Strategisk Forskning. P. Persson is acknowledged for stimulating discussions.

References and Notes

(1) Grätzel, M. *Prog. Photovoltaics* **2000**, *8*, 171.
(2) Hagfeldt, A.; Grätzel, M. *Acc. Chem. Res.* **2000**, *33*, 269.
(3) Nazeeruddin, M. K.; Kay, A.; Rodicio, I.; Humphry-Baker, R.; Müler, E.; Liska, P.; Vlachopoulos, N.; Grätzel, M. *J. Am. Chem. Soc.* **1993**, *115*, 6382.
(4) Nazeeruddin, M. K.; Pechy, P.; Grätzel, M. *Chem. Commun.* **1997**, 1705.
(5) Finnie, K. S.; Bartlett, J. R.; Woolfrey, J. L. *Langmuir* **1998**, *14*, 2744.
(6) Shklover, V.; Ovchinnikov, Y. E.; Braginsky, L. S.; Zakeeruddin, S. M.; Grätzel, M. *Chem. Mater.* **1998**, *10*, 2533.
(7) Rensmo, H.; Westermark, K.; Södergren, S.; Kohle, O.; Persson, P.; Lunell, S.; Siegbahn, H. *J. Chem. Phys.* **1999**, *111*, 2744.
(8) Fillinger, A.; Parkinson, B. A. *J. Electrochem. Soc.* **1999**, *146*, 4559.
(9) Persson, P.; Lunell, S. *Sol. Energy Mater. Sol. Cells* **2000**, *63*, 139—148.
(10) Patthey, L.; Rensmo, H.; Persson, P.; Westermark, K.; Vayssieres, L.; Stashans, A.; Petersson, Å.; Brühwiler, P. A.; Siegbahn, H.; Lunell, S.; Mårtensson, N. *J. Chem. Phys.* **1999**, *110*, 5913.
(11) Schnadt, J.; Brühwiler, P. A.; Patthey, L.; O'Shea, J. N.; Södergren, S.; Odelius, M.; Ahuja, R.; Karis, O.; Bässler, M.; Persson, P.; Siegbahn, H.; Lunell, S.; Mårtensson, N. *Nature* **2002**, *418*, 620.
(12) Sandell, A.; Andersson, M. P.; Alfredsson, Y.; Johansson, M. K.-J.; Schnadt, J.; Rensmo, H.; Siegbahn, H.; Uvdal, P. *J. Appl. Phys.* **2002**, *92*, 3381.
(13) O'Regan, B.; Grätzel, M. *Nature* **1991**, *353*, 737.
(14) Brühwiler, P. A.; Karis, O.; Mårtensson, N. *Rev. Mod. Phys.* **2002**, *74*, 703.
(15) Westermark, K.; Rensmo, H.; Schnadt, J.; Persson, P.; Södergren, S.; Brühwiler, P. A.; Lunell, S.; Siegbahn, H. *Chem. Phys.* **2002**, *285*, 167.
(16) Andersen, J. N.; Björneholm, O.; Sandell, A.; Nyholm, R.; Forsell, J.; Thånell, L.; Nilsson, A.; Mårtensson, N. *Synchrotron Radiat. News* **1991**, *4* (4), 15.
(17) Nyholm, R.; Svensson, S.; Nordgren, J.; Flodström, A. *Nucl. Instrum. Methods A* **1986**, *246*, 267.
(18) Maxwell, A. J.; Brühwiler, P. A.; Arvanitis, D.; Hasselström, J.; Mårtensson, N. *Chem. Phys. Lett.* **1996**, *260*, 71.
(19) Schnadt, J.; O'Shea, J. N.; Patthey, L.; Krempaský, J.; Mårtensson, N.; Brühwiler, P. A. *Phys. Rev. B.* **2003**, *67*, 235420.
(20) Coville, M.; Thomas, T. D. *Phys. Rev. A* **1991**, *43*, 6053.
(21) Persson, P.; Stashans, A.; Bergström, R.; Lunell, S. *Int. J. Quantum Chem.* **1998**, *70*, 1055.
(22) Lazzeri, M.; Vittadini, A.; Selloni, A. *Phys. Rev. B* **2001**, *63*, 155409.
(23) Lazzeri, M.; Vittadini, A.; Selloni, A. *Phys. Rev. B* **2002**, *65*, 119901.
(24) Hebenstreit, W.; Ruzycki, N.; Herman, G. S.; Gao, Y.; Diebold, U. *Phys. Rev. B* **2000**, *64*, R16334.
(25) Hengerer, R.; Bolliger, B.; Erbudak, M.; Grätzel, M. *Surf. Sci.* **2000**, *460*, 162.
(26) Burnside, S. D.; Shklover, V.; Barbé, C.; Comte, P.; Arendse, F.; Brooks, K.; Grätzel, M. *Chem. Mater.* **1998**, *10*, 2419.
(27) Persson, P.; Lunell, S.; Brühwiler, P. A.; Schnadt, J.; Södergren, S.; O'Shea, J. N.; Karis, O.; Siegbahn, H.; Mårtensson, N.; Bässler, M.; Patthey, L. *J. Chem. Phys.* **2000**, *112*, 3945.
(28) In photoemission spectroscopy, shake-up structures appear as features at higher binding energies (and, hence, lower kinetic energies) than the main peaks, typically with a separation of a few tenths of an electron volt to several or some tens of electron volts from the main peak. They are a result of multielectron processes in which electrons are excited from the occupied valence orbitals to the unoccupied ones, thereby reducing the kinetic energy of the outgoing (and measured) photoelectron (cf. panel c in Figure 5 in this paper). An analysis of their energies and intensities can provide useful information, in particular, about the electronic structure and the screening properties of the probed system (see, for example, refs 29—31).
(29) Hüfner, S. *Photoelectron Spectroscopy*, 2nd ed.; Springer—Verlag: Berlin, 1996.
(30) Enkvist, C.; Lunell, S.; Svensson, S. *Chem. Phys.* **1997**, *214*, 123.
(31) Tillborg, H.; Nilsson, A.; Mårtensson, N. *J. Electron Spectrosc. Relat. Phenom.* **1993**, *62*, 73.
(32) Schnadt, J.; O'Shea, J. N.; Patthey, L.; Schiessling, J.; Krempaský, J.; Shi, M.; Mårtensson, N.; Brühwiler, P. A. *Surf. Sci.* **2003**, *544*, 74.
(33) We ascribe the observed change in shake-up energy between the two systems to a change in the dielectric screening. This screening would have to be supplied by the substrate and suggests that the permittivity and/or average separation between molecule and image plane is different for the two cases. For isotropic permittivities, the problem can be treated analytically by the method of images.[18,34,35] However, the permittivities of both anatase and rutile are anisotropic. For the rutile single crystal,[36] $\epsilon_c = 170$ and $\epsilon_a = 86$, whereas, for thin films of anatase, permittivites have been measured that differ very much with the exact preparation method.[37,38] However, it is likely that the permittivity of anatase could reach values similar to that of rutile.[38] Although the present knowledge is not sufficient for a quantitative evaluation of the substrate screening responses, it can be

noted that the intramolecular charge-transfer character of the shakeup will lead to different responses for the shake-up final state and the main line, and that these, generally, are different for the different substrates. The explanation is also consistent with the XAS result that the orbitals are quite similar for the two cases.

(34) Durand, E. *Electrostatique. Tome III. Méthodes de Calcul Diélectriques*; Masson et Cie: Paris, 1966; pp 232−233.

(35) Chiang, T.-C.; Kaindl, G.; Mandel, T. *Phys. Rev. B* **1986**, *33*, 695.

(36) Parker, R. A. *Phys. Rev.* **1961**, *124*, 1719.

(37) Park, B. H.; Li, L. S.; Gibbons, B. J.; Huang, J. Y.; Jia, Q. X. *Appl. Phys. Lett.* **2001**, *79*, 2797.

(38) Fukuda, H.; Namioka, S.; Miura, M.; Ishikawa, Y.; Yoshino, M.; Nomura, S. *Jpn. J. Appl. Phys.* **1999**, *38*, 6034.

(39) The parameter τ_C is equal to Planck's constant ($\hbar$) times the inverse of the natural width Γ of the corresponding core level. For an N 1s core hole, Γ lies in the range of 0.09 eV (calculated for a single N atom) to 0.12 eV (for N_2) and 0.14 eV (for NO, found both theoretically and experimentally[20]), resulting in τ_C values of 7.3, 5.5, and 4.7 fs. N and NO represent extreme cases, in terms of the local valence population on the N atom. Because this population is responsible for the exact value of the lifetime, the given values should represent the approximate range of possible N 1s core-hole lifetimes. Therefore, we use a value of $\tau_C = 6$ fs, which is the mean value of the numbers given previously.

(40) Schnadt, J.; O'Shea, J. N.; Patthey, L.; Kjeldgaard, L.; Åhlund, J.; Nilson, K.; Schiessling, J.; Krempaský, J.; Shi, M.; Karis, O.; Glover, C.; Siegbahn, H.; Mårtensson, N.; Brühwiler, P. A. *J. Chem. Phys.* **2003**, *119*, 12462.

(41) For an isolated excited state, the RPES signal disperses linearly on the binding energy scale, by virtue of energy conservation, if the experiment is conducted using narrow-band excitation, i.e., using a photon resolution below the lifetime broadening of the excited state (see, for example, ref 14). The experiment is said to be conducted under Auger resonant Raman (ARR) conditions. Even then, the *overall* dispersion across the entire spectral range is zero for two or more energetically well-separated excited (electronic) states (not coupled to any continuum), whereas it is linear within each resonance. Finally, for excited states with overlapping tails (commonly vibrational states), interference effects that destroy the linear dispersion might be present (see, for example, ref 42). In principle, the present experiment could be conducted using both narrow-band or broad-band excitation, and, in both cases, the *overall* zero dispersion can be used to distinguish RPES and RAES features, because several well-separated electronic resonances are part of the experiment's spectral range.

(42) Piancastelli, M. N. *J. Electron Spectrosc. Relat. Phenom.* **2000**, *107*, 1.

(43) A normalization using a gas-phase measurement truly representing the isolated molecule would be ideal but, however, is not easily conducted, because of the low vapor pressure of BINA.

(44) Persson, P.; Lunell, S.; Ojamäe, L. *Chem. Phys. Lett.* **2002**, *364*, 469.

(45) Odelius, M.; Persson, P.; Lunell, S. *Surf. Sci.* **2003**, *529*, 47.

(46) Wurth, W.; Menzel, D. *Chem. Phys.* **2000**, *251*, 141.

(47) See, e.g., ref 50.

(48) Menzel, D.; Rocker, G.; Steinrück, H.-P.; Coulman, D.; Heimann, P. A.; Huber, W.; Zebisch, P.; Lloyd, D. R. *J. Chem. Phys.* **1992**, *96*, 1724.

(49) Mauerer, M.; Zebisch, P.; Weinelt, M.; Steinrück, H.-P. *J. Chem. Phys.* **1993**, *99*, 3343.

(50) Dudde, R.; Rocco, M. L. M.; Koch, E. E.; Bernstorff, S.; Eberhardt, W. *J. Chem. Phys.* **1989**, *91*, 20.

(51) In the present case, the photon energy for a N KVV Auger measurement is restricted to values between ∼410 eV (immediately above the N K-edge) and 455 eV. For higher energies, the Ti 2p threshold is crossed and the Ti LVV Auger at exactly the same kinetic energy renders direct measurement of the N Auger spectrum impossible. For photon energies between these values, strong, direct photoemission signals are always present in the spectra: Ti 3p and Ti 3s with rich shake-up structures, and O 1s excited with second-order light. To circumvent this problem, the Ti 3s core level has been measured at ∼75 different photon energies that are relevant for an N Auger measurement, thus forming an envelope of the latter.[40] The present curve has been extracted from these data.

(52) Brühwiler, P. A.; Maxwell, A. J.; Mårtensson, N. *Int. J. Mod. Phys. B* **1992**, *6*, 3923.

(53) Stier, W.; Prezhdo, O. V. *J. Phys. Chem. B* **2002**, *106*, 8047.

(54) Schnadt, J.; Schiessling, J.; Brühwiler, P. A. submitted to *Phys. Rev. B*.

(55) Lanzafame, J. M.; Palese, S.; Wang, D.; Miller, R. J. D.; Muenter, A. A. *J. Phys. Chem.* **1994**, *98*, 11020.